Journal of Applied Sciences and Nanotechnology

Journal homepage: jasn.uotechnology.edu.iq

Dielectric Properties of Surface-Doped Partially Stabilised Zirconia with Ceramic Nanomaterials

Lara Abd Al-Hakeem*, Shihab A. Zaidan, Wafaa Khalid Khalef

College of Applied Sciences, University of Technology-Iraq, Iraq

A R T I C L E I N F O

Article history:
Received: July, 01, 2025
Accepted: December, 09, 2025
Available online: December, 10, 2025

Keywords:
Dielectric constant,
AC conductivity,
Electrical breakdown,
Weibull modulus,
Energy Storage

Corresponding Author:
Lara Abd Al-Hakeem
lara1995hakeem@gmail.com

A B S T R A C T

The microstructural and dielectric properties of Yttria-partially stabilized zirconia (Y-PSZ) were studied before and after sintering with $BaTiO_3$ and WO_3 doping. After sintering, FE-SEM analysis revealed increased grain coalescence and growth, with $BaTiO_3$ causing 300 nm grain expansion and WO_3 promoting uniform grain distribution without significant grain size increase (~200 nm). These microstructural changes dramatically altered dielectric behavior. All sintered samples had higher dielectric constants than pre-sintered ones between 100–1000 kHz due to reduced porosity and enhanced homogeneity. Dielectric constant was highest in $BaTiO_3$-doped Y-PSZ at lower frequencies, while WO-doped showed superior frequency stability and lower dielectric loss across the spectrum. In doped crystals, sintering increased crystallinity, lowered defects, and lowered polarization losses. Dielectric loss (tan δ) varied with frequency, with $BaTiO_3$ showing higher losses at low frequencies and showing more stability at higher frequencies, while WO_3 showed a moderate, consistent loss. Sintering enhances AC conductivity, especially in $BaTiO_3$-doped materials, via enhancing charge mobility through structural alignment and crystallinity. Due to fault-localized field concentrations, higher voltage increase rates (VIR), lower Weibull modulus and electrical breakdown strength. $BaTiO_3$ and WO_3 doping improved grain bonding, void filling, dielectric strength, and energy storage. Tradeoffs between dielectric constant and breakdown strength. High dielectric constants decreased breakdown strength and vice versa. WO-doped Y-PSZ exhibited the highest energy density (22.86 kJ/m^3), followed by $BaTiO_3$ (15.22 kJ/m^3) and unaltered sintered (14.24 kJ/m^3). These investigations demonstrate that alterations to microstructure and the incorporation of impurities improve the energy storage capacity and high-frequency performance of dielectric materials.

https://doi.org/10.53293/jasn.2025.7802.1348, Department of Applied Sciences, University of Technology - Iraq.

1. Introduction

Partially Stabilised Zirconia (PSZ) with considerable characteristics is a suitable alternative for applications that require high-quality dielectric materials, especially at high temperatures [1]. The material's crystal structure, chemical composition, and electrical conductivity all work together to make it a good dielectric [2]. The different

amounts of partial stabilisation in zirconia change its electrical properties, and this is a big part of what makes them better. Zirconia's crystal structure becomes more stable when you add Y_2O_3 (Y-PSZ) or another oxide to it. This addition stops phase fluctuations that affect how well electrical insulation works. Partial stabilisation also changes the electrical polarisation of the material, which slows down the passage of charge and raises the dielectric constant. This makes zirconia a better insulator [3]. **Fig. 1** shows the empty spaces that form in the structure when the yttrium ion replaces the zirconium ion. When the electric field is turned on, the positive ions move toward the field and the negative ions move away from it. This movement creates dipoles, which then cause electrical polarisation. Space charge polarisation happens when there are empty spaces, especially at low frequencies [4].

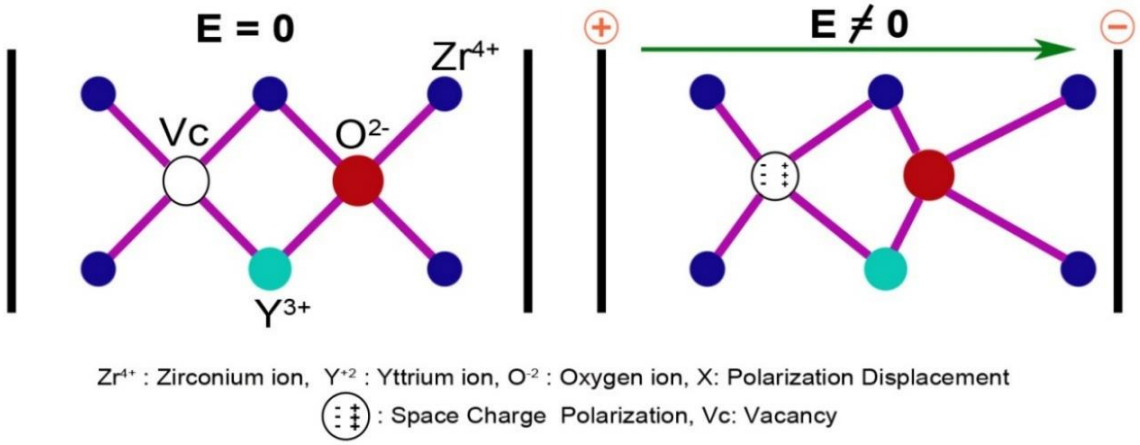

Figure 1: Mechanism of electrical polarisation in Y-PSZ ceramics.

Surface doping of partially stabilised zirconia is especially important for making zirconia's dielectric characteristics better. Adding particular metals or minerals to the surface of zirconia is called "surface doping." This changes how the charges in the materials interact with each other, which changes how well they work electrically. For instance, doping can change the dielectric constant of zirconia by changing how much energy it absorbs and how charges travel through it. This makes the material better for use in electronics and electricity. In general, surface doping of zirconia does the following [5]:

- Enhancing the dielectric properties of zirconia to provide a better electrical insulator.
- Changing the quantity of charges in the material and how they move, which changes how well it conducts electricity and how polarised it is.
- Keep the material stable when it is used in different situations, such as when it is hot or in strong electric fields.

Doping partly stabilised zirconia (Y-PSZ) with barium titanate ($BaTiO_3$) modifies the dielectric characteristics in intricate manners. When heavier ions, such as zirconium in $BaTiO_3$, take the place of Zr^{4+} sites, the crystal lattice parameters get bigger and the cubic phase stability is better. On the other hand, adding Ba^{2+} and Ti^{4+} to the zirconia lattice could change the Y-PSZ structure. It depends on how much is added whether the tetragonal or cubic phases are more stable [6]. In Y-PSZ, $BaTiO_3$ additions may separate at grain boundaries, which slows down grain growth and improves the microstructure, like in systems with zirconium oxide-doped $BaTiO_3$. Adding zirconia to $BaTiO_3$ - ZrO_2 composites lowers the dielectric constant, but it makes the material more stable at high temperatures. Y-PSZ has zirconium oxide in it; therefore, it might have the same trade-offs. For example, employing Ti^{4+} instead of ZrO_2 may lower the electrical permittivity since Ti^{4+} is less polar than Zr^{4+}. On the other hand, charge imbalance, like when Ba^{+} takes the place of Zr^{4+}, could generate oxygen vacancies that make electrical loss worse [7]. Depending on the Ti/Zr ratio, the dielectric constant of Y-PSZ with $BaTiO_3$ added may be lower than that of pure Y-PSZ. This also keeps the dielectric's properties stable at high temperatures, which is what happens in $BaTiO_3$ - ZrO_2 systems [8, 9].

In addition, the high concentrations of oxygen vacancies cause larger dielectric loss, which reveals the necessity of compensatory doping (such as donor-acceptor co-doping) [10]. Adding tungsten oxide (WO_3) to zirconia makes it more stable and has a big effect on its dielectric characteristics. Adding tungsten oxide to zirconia usually improves its structure and physical properties, resulting in increasing its resistance to electricity and improving its insulating electrical properties [11]. Doping enlarges the granules on the surface of the material and uniformly distributes them, thereby enhancing insulating electrical [12]. Adding tungsten oxide also makes the crystalline structure of zirconia less defective, which lowers unwanted electrical conductivity and raises the material's electrical resistance. Researchers have demonstrated that doping zirconia with tungsten oxide partially stabilises it and enhances its dielectric characteristics through many mechanisms, including increasing crystal stability, minimising flaws, and promoting grain growth. The modifications to the microstructure improve the material's insulating properties and make it less likely to conduct electricity [11, 13].

2. Dielectric Properties

2.1. Dielectric Constant

The internal electric field of a substance can tell you how well it can store electrical energy. This feature, which depends on the material's atomic structure and composition, is shown by the symbol (ε′). The device used operates at a maximum frequency of 1 MHz. While the results might differ at higher frequencies, the test was conducted within the operating limits of the available laboratory equipment. Ceramics are characterised by an atomic structure of ionic or covalent bonds that prevent the movement of free electrons, making them poor electrical conductors and excellent insulators. The dielectric constant of ceramics is affected by several factors, including temperature. Ceramics can maintain their dielectric constant at higher temperatures than other materials. The thickness of the dielectric (d) plays a role in the charge distribution within the material, as optimal thickness promotes uniform charge distribution and reduces electric field heterogeneity. The dielectric constant is described by **Eq. (1)**:

$$\boldsymbol{\varepsilon' = \frac{C_p \,.\, d}{\epsilon_o \,.\, A}} \qquad (\mathbf{1})$$

Where: Cp is the capacitance with dielectric materials, ϵo is the space permittivity (8.85×10^{-12} F/m)
A: is the area of the specimen surface [14].

2.2. Dielectric Loss: or Loss Factor (tan δ)

A measure of the energy lost in an insulating material when exposed to an alternating electric field. It expresses the ratio of the energy lost to the stored energy. Dielectric loss is affected by frequency, temperature, humidity, the presence of impurities or defects in the material, and changes in thickness [15]. Increased temperature and humidity lead to increased dielectric loss due to increased movement of ions or impurities within the ceramic [16]. High frequency leads to a change in the polarisation properties within the material, affecting dielectric loss [15].

2.3. Alternating Conductivity (AC)

A measure of the insulator's ability to transmit alternating electrical current. It differs from direct conductivity (DC) since it is strongly influenced by the frequency of the applied electrical current. The AC electrical conductivity (γ_{AC}) of ceramic insulators is described by **Eq. (2)** [17]:

$$\boldsymbol{\gamma_{AC}(f) = 2\pi f \epsilon_o \epsilon' \, tan\delta} \qquad (\mathbf{2})$$

AC conductivity represents the power lost in a material due to the movement of charges or the rotation of dipoles within the insulator when the direction of an alternating electric field changes. It is therefore related to the amount of heat generated in the insulator [18]. Low AC conductivity in ceramic insulators indicates high dielectric quality and effective current suppression. Measuring AC conductivity can also reveal defects or changes in the internal structure of the insulator, such as gaps or heterogeneities, which affect the insulator's performance. AC conductivity is also important in insulator design because alternating currents are the most common in electrical power systems. The presence of gaps, impurities, or inhomogeneity in the material increases the AC conductivity due to facilitating the movement of charges or the presence of conductive paths within the insulator [19]. As the frequency increases, consequently, because charges can move freely, the AC conductivity of insulating materials

goes up [20]. Sintering at high temperatures makes the material denser and less porous, which in turn increases the AC conductivity of interfacial polarisation. Understanding how these things affect the materials makes sure they will last and work well [21].

2.4. Electrical Breakdown

Y-PSZ is used in a lot of different items that need strong mechanical and dielectric properties, such as making power tools and electrical insulators. Electrical breakdown strength is the ability of a material to stop the flow of electricity until the substance breaks down and shows conductivity. This happens when the material is exposed to high voltage. This feature is important for keeping zirconia's electrical performance steady and preventing surprise failures in real life, especially when the voltage or temperature is constantly changing [22]. Adding yttrium oxide or other stabilisers to zirconia changes the way the crystals are arranged, which makes it less likely to break down when electricity flows through it. This means that fewer crystallographic and internal flaws let the current leak out [23]. The electrical breakdown voltage is lower because of impurities and minor flaws in the materials. This makes the material weaker and makes it easier for the current to flow through it at high voltage. When the temperature is high, atoms move and vibrate a lot more, which makes it easier for current to flow and decreases the breakdown voltage [24]. Water or moisture on or in the material can lower the electrical breakdown voltage by creating conductive bridges between the electrodes. These bridges make it easier for current to pass and make the insulator weaker [25]. The breakdown voltage is affected by the geometry of the conducting electrode and the strength of the electric field [26]. Localised voltage concentrations induced by uneven field distribution can cause the early breakdown [27]. You may find the electrical breakdown strength (E_{br} in kV/mm) by looking at the highest voltage (V_{max}) that was applied to the insulator when it broke down as shown in **Eq. (3)** [19].

$$\boldsymbol{E_{br} = \frac{V_{max}}{d}} \quad (\mathbf{3})$$

3. Weibull statistical analysis

The electrical robustness of ceramics comes from the fact that they can handle high voltages without breaking. The samples have different resistance abilities because of variances in surface and crystalline defects and phase distribution. Applying Statistical analysis is necessary for a full knowledge of how insulating strength is spread out. The Weibull statistical model can be used to figure out how long an insulator is likely to last and how likely it is to break down in different operating situations. This is because the model evaluates the chance of an insulator failing at different voltage levels. This study offers significant insights into dependable ceramic insulators in practical applications [28]. Figuring out how likely it is that an insulator will fail at various voltages and in certain situations helps make insulation systems that are safer and work better.

Eq. (4) tells us how likely it is that a sample will survive without failing (Ps):

$$\boldsymbol{P_s = 1 - \frac{J}{N+1}} \quad (\mathbf{4})$$

Hence, J: rank of the sample and N: the total number of samples.

When studying electrical breakdown, the exponential equation **Eq. (5)** of the Weibull distribution is used to determine the probability of breakdown occurring at a given voltage. The most common form of the equation is:

$$\boldsymbol{P_s(E) = exp\left(-\frac{E_{br}}{E_{bro}}\right)^{\beta}} \quad (\mathbf{5})$$

Where: $P_s(E)$ is the probability that electrical breakdown will occur at or before a breakdown of E, E_{br}: the breakdown strength of applied voltage (or the value of the random variable), E_{bro}: the characteristic breakdown strength or Weibull scale parameter (the voltage at which a probability of breakdown of approximately 63.2% is achieved), and β: is Weibull modulus, which is a measure of data dispersion; a higher modulus indicates lower data dispersion [29]. **Fig. 2** shows the plot of the Weibull function for the statistical distribution according to **Eq.**

(5) for different values of the Weibull modulus. The best case for the data distribution is when the Weibull modulus is $\beta \geq 5$. The Weibull statistical method eliminates the need for the standard deviation, as it represents the extent of deviation from a specific value that characterises the material.

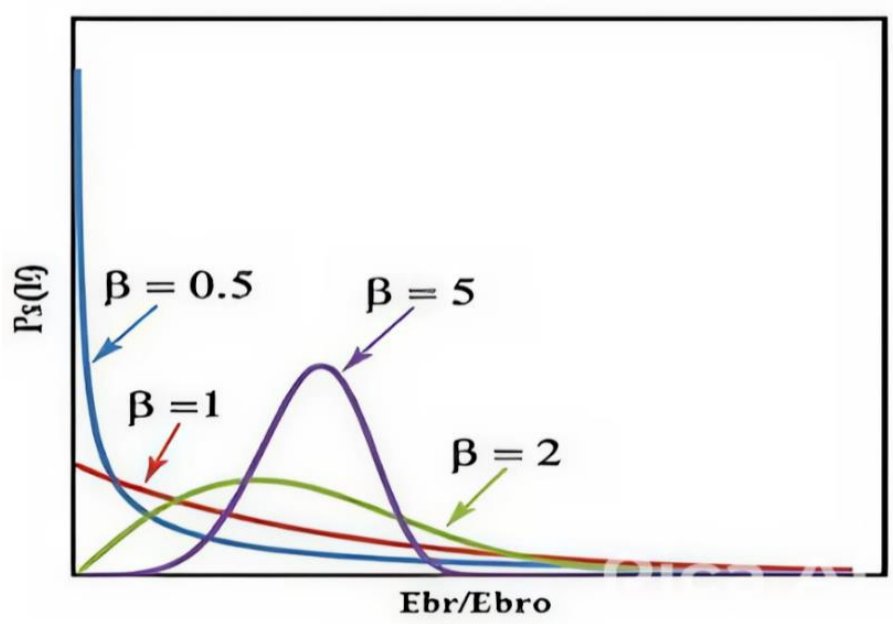

Figure 2: Statistical Weibull distribution for different Weibull modulus

Eq. (6) is the linear form of **Eq. (5)**:

$$ln\left(ln\left|\frac{1}{P_s(E)}\right|\right) = \beta\, ln\, E_{br} - \beta\, ln\, E_{bro} \qquad (6)$$

This figure allows you to plot the relationship between the X-axis: $ln\ E_{br}$ and the Y-axis: $ln\left(ln\left|\frac{1}{P_s(E)}\right|\right)$.

The resulting line will have a slope of β (the Weibull modulus), and the Y-intercept will give $\beta\, lnE_{bro}$.

4. Energy Storage

The concept of energy storage in electrical insulators, such as (Y-PSZ), relates to the ability of these materials to store electrical energy in the form of an electric field within the material when subjected to an electrical voltage. In general, electrical insulators store energy through electrical polarization, where electrical charges store potential energy that can be later released. Partially stabilized zirconia is an effective material in this field due to its physical and chemical properties that support its stability and efficiency in storing electrical energy. The basic relationship describing energy storage (E.S) per unit volume (J/m^3) in dielectrics comes from the physics of dielectric capacitors shown in **Eq. (7)** [30]:

$$E.S(J/m^3) = \frac{1}{2}\, \varepsilon_o\, \varepsilon'\, E_{br}^2 \ldots\ldots (7)$$

5. Materials and Methods

Chemical composition by weight of the pre-sintering Y-PSZ block used to prepare partially yttria-stabilized zirconia samples from (radiantprolab zirconia) is: $ZrO_2 + HfO_2 + Y_2O_3 \geq 99$ wt.%, where Y_2O_3 (yttria) ≈ 4.5 – 6.0 wt.%, Al_2O_3 (aluminum oxide): less than 0.25 wt.% % and other oxides (such as SiO_2, Fe_2O_3, CaO, etc.): less than 0.15 wt%. The specimens were designed and manufactured in the form of discs with a diameter of 20 mm and a thickness of 2 mm using CAD/CAM design software and a CNC milling machine.

Barium titanate ($BaTiO_3$: Cubic, SkySpring Nanomaterials USA, 99.9 %, 50-70 nm) and tungsten oxide (WO_3: Hongwunew material China 99.9% – 50nm) nanoparticles were used as the doping material, and the doping material- alcohol solution was prepared, and then the doping was performed by spin-coating method (2000 rpm for 30 s) on the Y-PSZ surface with 14 % Apparent Porosity.

After doping the surface of the Y-PSZ samples, the sintering process was completed at 1300 °C with a soaking time of 5 hours. **Fig. 3** shows the three stages of the doped sample preparation process. The first stage includes preparing the pre-sintered Y-PSZ samples, the second stage is the doping stage and finally the sintering stage.

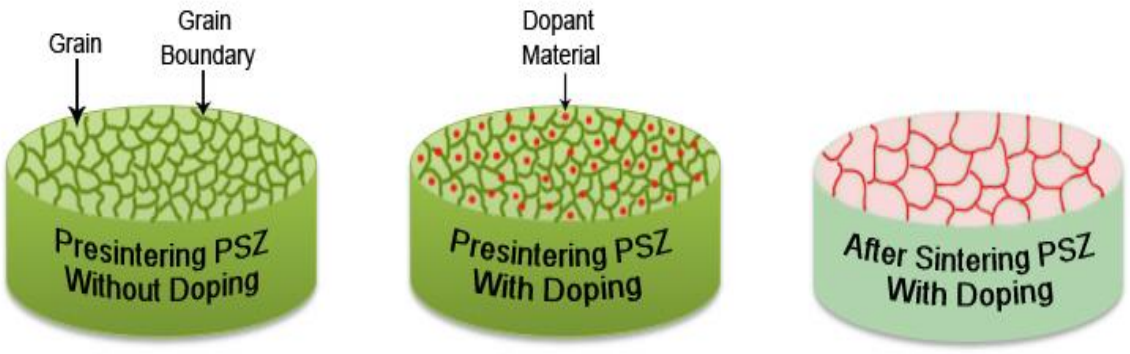

Figure 3: Three stages of the doped sample process.

The prepared samples were subjected to electrical insulation tests. The RLC device (micro test/LCR meter, model 6377 (0-1MHz) Taiwan) was used to perform the dielectric constant and dielectric loss tests. The dielectric strength was measured using the device (high-voltage supply, BAUR-PGO-S-3, German), with different voltage increasing rates (VIR) (0.5 and 5 kV/s).

6. Results and Discussion

6.1. Structural Properties

6.1.1. Field Emission-Scanning Electron Microscope (FE-SEM)

Surface morphology was studied using the FE-SEM technique. **Fig. 4a** shows the powder grain distribution before sintering (pre-sintered Y-PSZ samples). This indicates strong powder convergence and uniformity in the distribution of the pressed powder. This convergence helps achieve the powder particle coalescence process during the sintering process in a short time and at a low temperature. The average powder particle size can be estimated mathematically to be ~125 nm. **Fig. 4b** shows the surface of the sample after sintering, demonstrating the coalescence of the grains and the formation of grain boundaries. The average grain size can be estimated by ~200 nm.

Fig. 4c shows the increase in grain size and, consequently, the increase in grain size resulting from the $BaTiO_3$ doping of Y-PSZ, while simultaneously increasing the grain coalescence. $BaTiO_3$ doping can be described as accelerating sintering and grain growth. The average grain size is estimated to be ~300 nm. **Fig. 4d** shows the WO_3 doping of Y-PSZ, demonstrating a higher uniformity in the grain distribution than with $BaTiO_3$ doping. In addition to the discontinuity of grain growth (without changing the average grain size ~ 200 nm), this condition may be beneficial in terms of taking advantage of the intergranular boundaries to increase the interfacial electrical polarization [31].

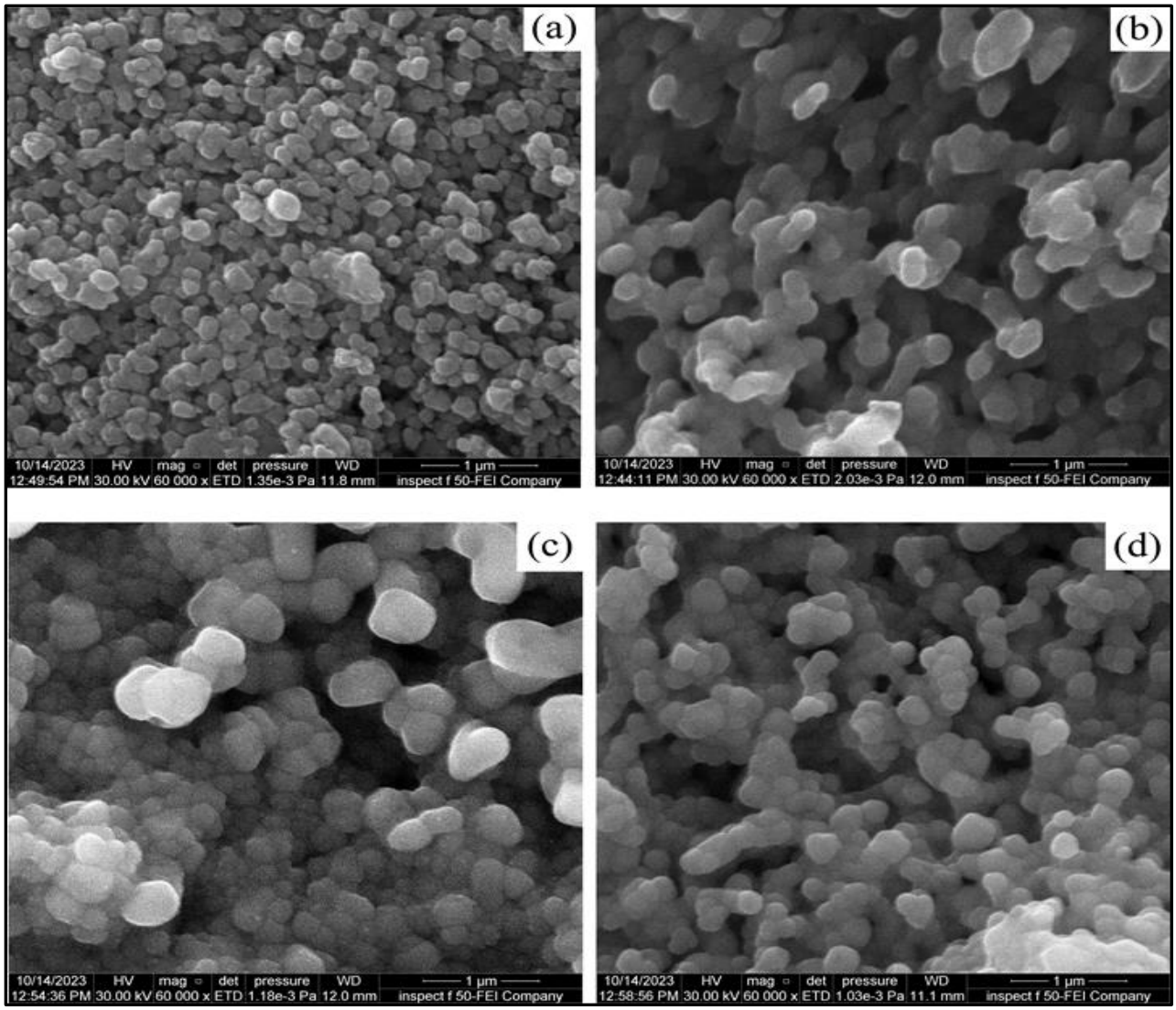

Figure 4: FE-SEM images of samples: (a) After sintering without additives, (b) before sintering without additives (c) $BaTiO_3$ - doped Y-PSZ and (d) WO_3 - doped Y-PSZ.

6.2. Dielectric Properties

6.2.1. Dielectric Constants

The dielectric constants were measured in the frequency range between 100 and 1000 kHz for $BaTiO_3$ and WO_3-doped Y-PSZ. **Fig. 5** shows the variation of the dielectric constant as a function of frequency for each dopant material. This result shows that all the samples exhibited the expected decline of the dielectric constant with increasing frequency, which is due to the decreasing contribution of some types of electric polarization in this frequency range, most notably space charge polarization. All sintered samples exhibit a higher dielectric constant compared to their presented sample; This may be related to decreased porosity and improvements in microstructural homogeneity that allow the material to polarize more effectively when an applied electric field [32]. Among those, $BaTiO_3$ and WO_3 have the highest dielectric constant at the lower frequency [33]; $BaTiO_3$ at the higher frequency maintains relatively high values, making it suitable for applications that require stable dielectric properties. Notably, above 400 kHz, a sharp decrease in the dielectric constant for all samples was observed; however, the presented samples depict a higher drop and therefore higher polarization losses due to defects and grain boundaries [34].

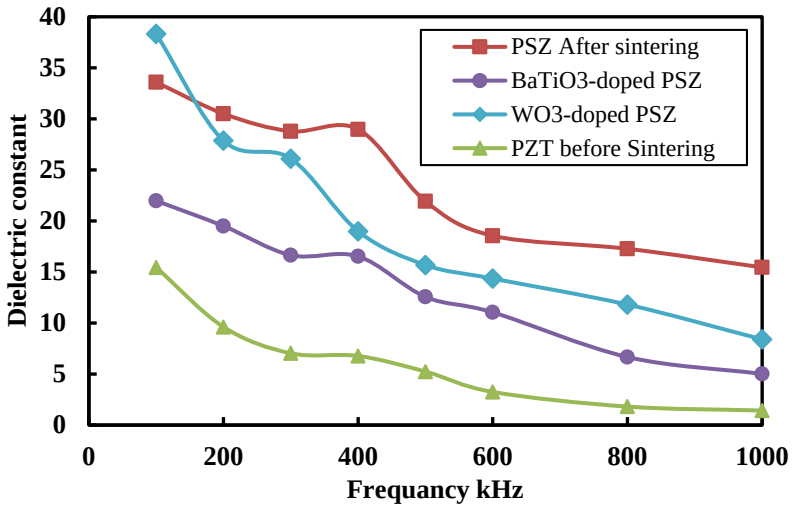

Figure 5: Dependence of dielectric constant on frequency for samples: Y-PSZ after and before sintering, $BaTiO_3$-doped Y-PSZ, WO_3-doped Y-PSZ.

These effects are minimized after sintering. While there is certainly a drop in the dielectric constant for all materials with the increasing frequency, sintering certainly improves the dielectric properties of all the studied materials, as these could be ideal for applications requiring high and stable dielectric constants over a wide frequency range [35]. Investigating the behavior of dielectric properties at elevated temperatures requires a specialized system, which is currently unavailable. Work will be conducted on this in the future.

6.2.2. Dielectric Loss (tan δ)

Dielectric loss (tan δ) in the frequency ranges from 100 to 1000 kHz for samples with various dielectric substances like $BaTiO_3$ -doped Y-PSZ, WO_3-doped Y-PSZ, as shown in **Fig. 6**. At low frequencies, $BaTiO_3$ has huge dielectric loss with a peak about 300 kHz, though this loss rapidly decreases as the frequency increases, indicating a very stable performance at higher frequencies. WO_3, though with a lower dielectric loss than $BaTiO_3$, has a linear dissipation trend throughout the frequency range and hence should be suitable for a wide frequency range with moderate energy retention, offering moderate energy retention and reliable applications, particularly at high frequencies. The sintering process and the type of dielectric material have great effects on the energy-dissipation behavior [36, 37].

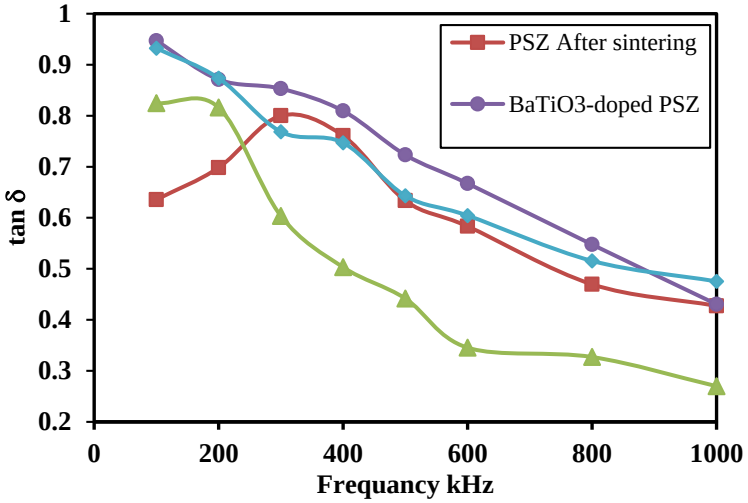

Figure 6: Dependence of Dielectric Loss (tan δ) on frequency for samples: Y-PSZ after and before sintering, $BaTiO_3$-doped Y-PSZ, WO_3-doped Y-PSZ.

The dielectric loss of Y-PSZ increases after sintering due to microstructural changes, particularly grain growth and reduced porosity. Grain coarsening decreases intergranular spacing, altering the material's response to electric fields and increasing energy dissipation. Additionally, reduced porosity enhances grain connectivity and leakage pathways, further contributing to dielectric loss [34]. However, after sintering, this decreasing porosity strengthens the structural bonding between the grains and enhances leakage current pathways, thus increasing the dielectric loss [38]. The increase in mobile ions resulting from sintering may lead to the release or increased concentration of ions such as O^{-2} or stabilized ions such as Y^{+3} in the crystal lattice. These ions may contribute to excessive polarization or small electric currents within the insulator, increasing dielectric loss. As for phase transformations in partially stabilized zirconia (monocline, tetragonal and cubic), sintering leads to greater stability of the tetragonal or cubic phases. These phases have different dielectric constants and may have higher losses compared to the monocline phase that prevailed before sintering [7]. Interfacial polarization (Maxwell-Wagner effect) after sintering also results in the appearance of more pronounced and coherent grain boundaries, which increase polarization effects at grain boundaries, especially at low frequencies, thus increasing dielectric loss [39].

6.2.3. AC Conductivity

AC conductivity for some obtained materials, like $BaTiO_3$, WO_3-doped Y-PSZ, was measured within the frequency range from 100 to 1000 kHz and shown in **Fig. 7**. In most cases, the AC conductivity with sintered materials displayed a high rise, but the most significant rises were observed in $BaTiO_3$ and WO_3-doped Y-PSZ. This enhancement could be attributed to crystallinity improving and reducing defect density after sintering, thus allowing easier movement of charge carriers. This could be due to resonance effects or proper alignment of dipoles within the materials at specific frequencies, especially for ferroelectric materials such as $BaTiO_3$ -doped Y-PSZ. In general, sintering increases the dielectric properties of all the materials studied here, but the conductivity of $BaTiO_3$-doped Y-PSZ was enhanced most of all, followed by that of WO_3-doped Y-PSZ. These findings underline that treatment techniques of materials are very important in their optimization concerning dielectric features, especially when aiming to use them in electronic devices as media that exhibit high conductivity at specific frequencies [40, 41].

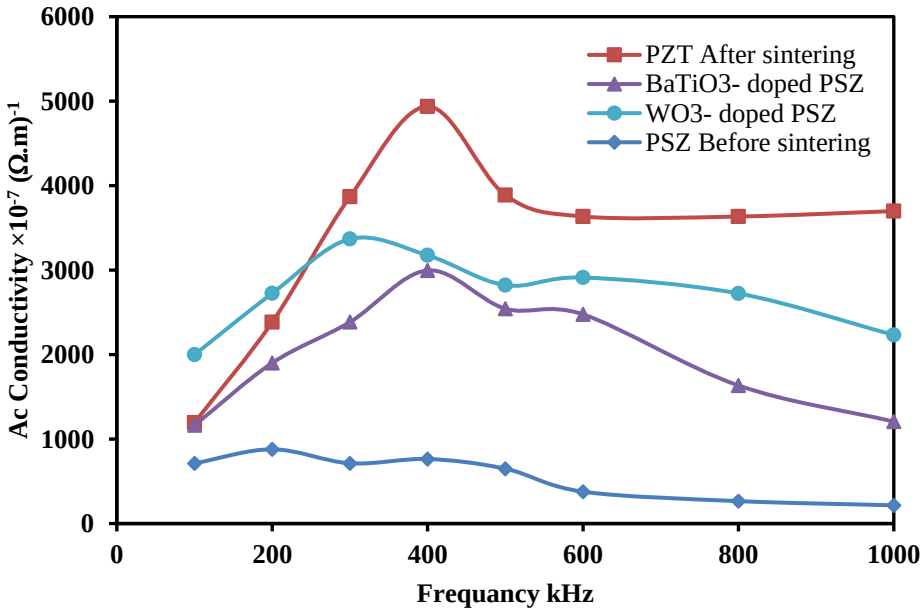

Figure 7: Dependence of AC Conductivity on frequency for samples: Y-PSZ after and before sintering, $BaTiO_3$-doped Y-PSZ, WO_3-doped Y-PSZ.

Increasing the AC electrical conductivity of dielectrics has some advantages, which include improving some operational properties at certain frequencies: Increasing AC conductivity may indicate the insulator's ability to adjust alternating currents, which can be useful in some electrical applications that rely on variable frequencies [42]. It is also an indicator of dipole polarization, as AC conductivity reflects the rotation of dipoles or the vibration of charges with the changing direction of an alternating field. This can help understand and improve dielectric properties. The disadvantages of increasing AC conductivity include increased leakage current through the insulator, leading to energy loss and increased heat generated within the insulator. It also accelerates insulator deterioration, as leakage currents and the resulting heat degrade the insulator over time, reducing its lifespan and increasing the likelihood of electrical faults. Furthermore, increasing conductivity leads to a decrease in the insulator's resistance, making the insulator less effective at preventing the passage of unwanted electrical current. High conductivity means greater electrical loss, resulting in lower electrical system efficiency and increased energy consumption. Generally, increased AC electrical conductivity of insulators means deterioration in electrical insulation performance, increased heat loss, and reduced service life, despite some limited benefits in special applications that rely on variable frequencies [43].

Electrical breakdown testing assesses a dielectric's tolerance to electric fields before energy gap failure. Electrical strength can be adopted as a criterion for the homogeneity of the distribution of Tungsten Oxide nano powder in the polyester matrix.

This can be evaluated using the Weibull statistical distribution, by which the Weibull modulus is determined, which expresses the convergence or divergence of the test results [28, 44]. **Fig. 8a and b** show that the sintered Y-PSZ sample exhibited a high Weibull modulus of 7.12 at VIR of 0.5 kV/s, which means a high homogeneity of the grain distribution of the Y-PSZ material during the forming processes. But it decreased to 4.37 at a VIR of 5 kV/s. **Fig. 8c and d** illustrate the changes in the survival probability of electrical breakdown strength for Y-PSZ after sintering with doping $BaTiO_3$ at a low VIR of 0.5 kV/s. This indicates that the electrical breakdown is related to the electrothermal changes that are associated with the breakdown that occurs as a result of the higher temperature that is associated with the applied voltage [45]. The Weibull modulus was calculated based on the slope of the straight line, with a value of 5.43. As the VIR continues to increase at 5 kV/s, the Weibull modulus decreases to 5.12. **Fig. 8 e and f** shows the alteration in the survival probability of electrical breakdown strength for WO_3 doped - Y-PSZ at VIR 0.5 kV/s. The Weibull modulus was determined from the slope of the straight line, with a value of 5.39, and the Weibull modulus decreases to 5.03 at VIR 5 kV/s. The Weibull modulus in dielectric strength testing decreases at high voltage due to the concentration of the electric field on small defects (such as impurities or microscopic voids), which leads to random and inconsistent activation. This also prevents the reorganization of electrical charges within the dielectric, increasing the likelihood of sudden and unexpected breakdowns.

6.3. Weibull Modulus

All Weibull modulus values and the typical strength value of the electrical field (Ebro: the characteristic breakdown strength) are listed in **Table 1**. Generally, dielectric strength decreases at low VIR due to increased leakage currents and heat generation from the dielectric, leading to premature electrical breakdown. The dielectric strength is also improved with $BaTiO_3$ and WO_3 doping due to the filling of interfacial voids and treatment of surface defects, in addition to the doping materials having good insulating properties.

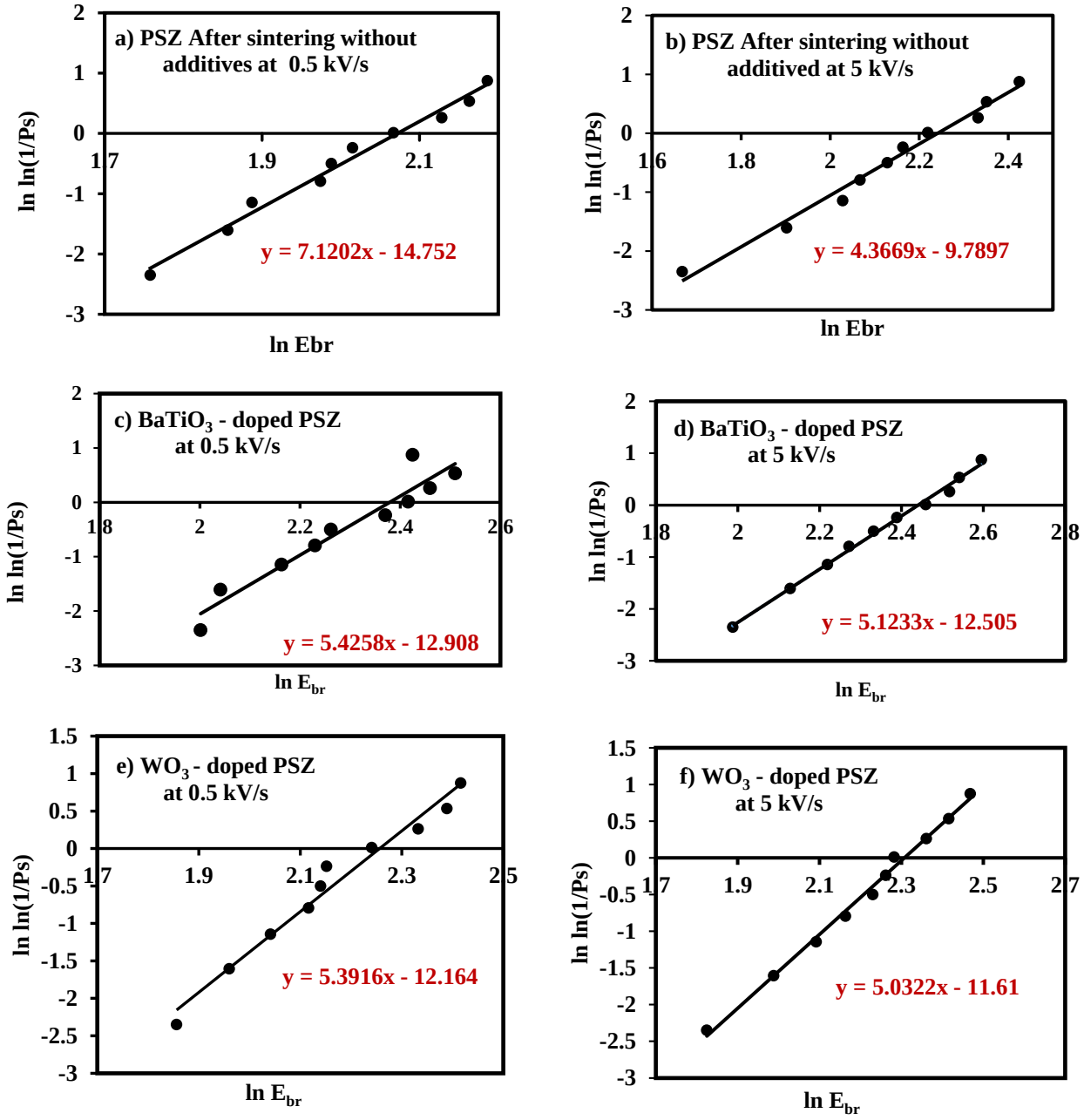

Figure 8: Weibull Distribution of Electrical Breakdown Strength for: (a, b) after sintering without additives at 0.5 kV/s and 5 kV/s, (c, d) $BaTiO_3$-doped Y-PSZ at 0.5 kV/s and 5 kV/s, (e, f) WO_3-doped Y-PSZ at 0.5 kV/s and 5 kV/s.

Table 1: Weibull Modulus β and Characteristic breakdown strength (E_{bro}) kV/mm of samples with different VIR.

Specimen	At 0.5 kV/s		At 5 kV/s	
	β	(E_{bro}) kV/mm	β	(E_{bro}) kV/mm
Y-PSZ After sintering without additives	7.12	7.94	4.37	9.40
$BaTiO_3$ - doped Y-PSZ	5.43	10.78	5.12	11.51
WO_3 – doped Y-PSZ	5.39	9.55	5.03	10.06

Eq. (7) is used to calculate the ability of an insulator to store energy per unit volume. It shows that the two main factors affecting the amount of stored energy are the dielectric constant (ε′) and the characteristic breakdown strength (E_{bro}) applied to the dielectric.

The results shown in **Fig. 9** illustrate the maximum values of the stored energy, calculated from the maximum field condition (dielectric strength) at a high voltage rate rise of 5 kV/s, and calculating the dielectric constant at low frequencies (100 kHz). Most of the electrical insulators, including those presented in the research, behave in a contradictory manner between electrical breakdown and dielectric constant.

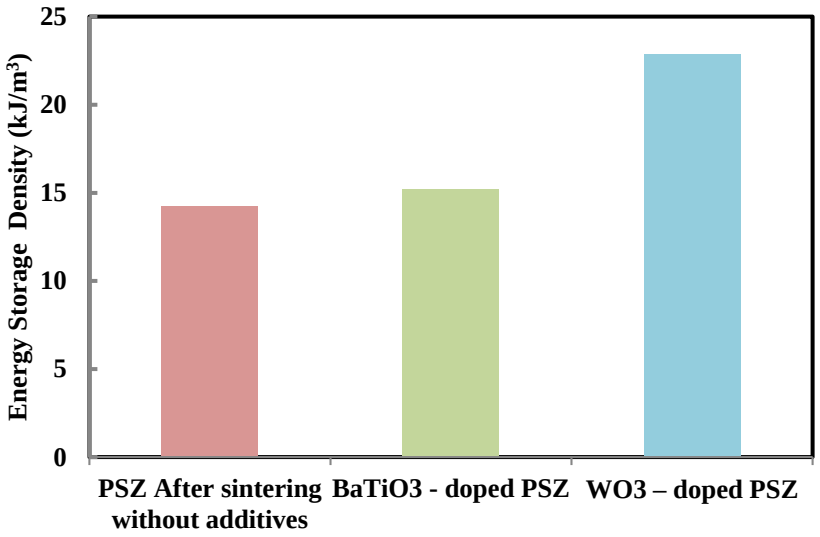

Figure 9: Energy Storage Density of samples.

In other words, an increase in the dielectric constant associated with the response of the dielectric material to the applied field, through electrical polarisation, is matched by a decrease in the dielectric strength, and vice versa. Therefore, a state of competition occurs: which factor has a stronger influence on changing the amount of stored energy, is it (ε′) or (E_{br}). According to **Eq. (2)**, the field strength is quadratic (E^2) and therefore will prevail, unless the dielectric constant reaches very high values. The stored energy value of the Y-PSZ sample after sintering is (14.24 kJ/m^3), due to the low values of (ε′) and (E_{bro}). While the stored energy value of the samples' sintering increased significantly up to (15.22 kJ/m^3) for $BaTiO_3$–doped Y-PSZ due to the dielectric strength increase. However, doping Y-PSZ with the addition of tungsten oxide (WO_3) showed the maximum value of the stored energy density (22.86 kJ/m3), as a result of the effect of the increase in the dielectric constant (**Table 2**).

Generally, a decrease in the stored energy density in a doped dielectric material means a decrease in the insulator's ability to retain electrical energy for a longer period of time. So, the ability to dissipate electrical energy is represented by the dielectric loss coefficient (tan δ), an increase in which leads to a decrease in the dielectric strength and, consequently, a decrease in the stored energy density [46].

Table 2: Compared with your gas sensing zirconia study.

Aspect	Dielectric Properties Study	Your Gas Sensing Study
Material Base	Yttria-partially stabilized zirconia (Y-PSZ)	Pure ZrO_2, MoO_3-doped ZrO_2, PZT-doped ZrO_2
Purpose	Improve dielectric performance & energy storage	Improve sensitivity/selectivity for toxic gas detection
Dopants	$BaTiO_3$, WO_3	MoO_3, PZT
Key Characterizations	FE-SEM, dielectric constant/loss, AC conductivity, Weibull analysis, energy storage	AFM, gas sensing response, sensitivity %, response/recovery time

Performance Metrics	Dielectric constant (ε), breakdown strength (E_{br}), energy density (kJ/m^3)	Sensitivity %, response/recovery time, gas selectivity
Findings	WO_3 improved dielectric constant & energy density (22.86 kJ/m^3), $BaTiO_3$ improved breakdown strength	PZT best for H_2S (S%=151.7), MoO_3 best for NO_2 (S%=24.2)

7. Conclusions

This study highlighted the effects of sintering and doping on the microstructure and dielectric performance of Y-PSZ ceramics. Sintering improved grain coalescence, reduced porosity, and enhanced crystallinity, leading to better dielectric behavior but also increased dielectric loss due to grain growth and leakage paths. Doping with $BaTiO_3$ promoted grain growth and increased breakdown strength, while WO_3 maintained uniform grain distribution and enhanced the dielectric constant without significant grain enlargement. All doped and sintered samples exhibited higher dielectric constants at low frequencies and improved AC conductivity, especially with $BaTiO_3$, due to better dipole alignment. However, dielectric loss and conductivity must be carefully controlled, as excessive values can degrade insulation performance and reduce energy storage capability. Weibull analysis confirmed improved grain uniformity at lower voltage rise rates, with a decline in dielectric strength at higher rates due to field concentration on defects. Energy storage density was highest in WO_3-doped Y-PSZ, driven by a high dielectric constant, while $BaTiO_3$-doped samples benefited from greater breakdown strength. In summary, both sintering and selective doping enhance the electrical performance of Y-PSZ ceramics, but optimization requires balancing dielectric constant, breakdown strength, and dielectric loss for targeted applications in electronic and energy storage systems. One of the advantages of ceramic materials is their low sensitivity to environmental conditions; therefore, this aspect was not a major focus of our study, despite the possibility of some minor changes.

Conflict of Interest

The authors declare that they have no conflict of interest.

References

[1] A. I. B. Rondão, J. P. F. Grilo, M. Starykevich, D. M. C. Dias, and F. M. B. Marques, "High temperature ionic and electronic conductivity in MgPSZ," *Solid State Ionics*, vol. 385, p. 116009, 2022.

[2] S. Alraddadi, "Crystal Structure, Microstructure, and Dielectric and Electrical Properties of Ceramic Material Prepared Using Volcanic Ash," *Crystals*, vol. 14, no. 9, p. 817, 2024.

[3] L. Gao, Y. Shao, Y. Xin, D. Yang, H. Zhang, M. Zhu, *et al.*, "Influence of Y_2O_3 Doping on Phase Evolution and Dielectric Characteristics of ZrO_2 Ceramics," *Micromachines*, vol. 15, no. 8, p. 938, 2024.

[4] M. Biswas, "Debye-type relaxation in yittria stabilized zirconia," *J. Alloys Compd.*, vol. 491, no. 1–2, pp. 30–35, 2010.

[5] G. Dutta, "A first-principles study of the effects of Hf doping on the dielectric response in ZrO_2," *J. Appl. Phys.*, vol. 105, no. 10, 2009.

[6] O. A. A. Abdelal, K. I. Othman, and E. S. Elshazly, "Stabilizing the Barium Titanate by Different Kinds of Zirconia," *Int. J. Sci. Eng. Res.*, vol. 5, no. 11, p. 85, 2014.

[7] M. Kurumada, H. Hara, and E. Iguchi, "Oxygen vacancies contributing to intragranular electrical conduction of yttria-stabilized zirconia (YSZ) ceramics," *Acta Mater.*, vol. 53, no. 18, pp. 4839–4846, 2005.

[8] N. M. Molokhia and M. A. Issa, "Dielectric properties of $BaTiO_3$ modified with ZrO_2," *Pramana*, vol. 11, no. 3, pp. 289–293, 1978.

[9] V. Buscaglia, M. T. Buscaglia, and G. Canu, "$BaTiO_3$-based ceramics: fundamentals, properties and applications," 2021, *Elsevier Oxford*.

[10] V. Paunović, Z. Prijić, and V. V Mitić, "Effect of donor and acceptor dopants on the microstructure and dielectric properties of barium titanate based ceramics," *Sci. Sinter.*, vol. 54, no. 1, pp. 81–91, 2022.

[11] S. R. Whitman and K. S. Raja, "Formation and electrochemical characterization of anodic ZrO_2–WO_3 mixed oxide nanotubular arrays," *Appl. Surf. Sci.*, vol. 303, pp. 406–418, 2014.

[12] L. Mahnicka-Goremikina, R. Svinka, and V. Svinka, "Influence of ZrO_2 and WO_3 doping additives on

the thermal properties of porous mullite ceramics," *Ceram. Int.*, vol. 44, no. 14, pp. 16873–16879, 2018.
[13] S. Triwahyono, A. A. Jalil, H. A. Azman, and C. R. Mamat, "Isomerization of C5-C7 Linear Alkanes over WO_3-ZRO_2 under Helium Atmosphere," *J. Teknol. (Sciences Eng.*, vol. 75, no. 6, 2015.
[14] J. Martinez-Vega, *Dielectric materials for electrical engineering*. John Wiley & Sons, 2013.
[15] Y. M. Poplavko, *Electronic materials: principles and applied science*. Elsevier, 2018.
[16] M. A. Mir, M. A. Shah, and P. A. Ganai, "Dielectric study of nanoporous alumina fabricated by two-step anodization technique," *Chem. Pap.*, vol. 75, no. 2, pp. 503–513, 2021.
[17] M. M. Mahmoud, A. Bhalla, N. P. Bansal, J. P. Singh, R. H. R.Castro, N. J. Manjooran, *et al.*, Eds., *Processing and Properties of Advanced Ceramics and Composites VII*. in Ceramic Transactions Series. Wiley, 2015. doi: 10.1002/9781119183860.
[18] A. S. Das and D. Biswas, "Investigation of Ac conductivity mechanism and dielectric relaxation of semiconducting neodymium-vanadate nanocomposites: temperature and frequency dependency," *Mater. Res. Express*, vol. 6, no. 7, p. 75206, 2019.
[19] J. Kuffel and P. Kuffel, *High voltage engineering fundamentals*. Elsevier, 2000.
[20] S. Dhiman, R. Meena, N. Manyani, and S. K. Tripathi, "Investigating the temperature and frequency dependence of dielectric response using AC impedance spectroscopy on SnO_2," *Surfaces and Interfaces*, vol. 42, p. 103362, 2023.
[21] H. Naceur, A. Megriche, and M. El Maaoui, "Effect of sintering temperature on microstructure and electrical properties of $Sr_{1-x}(Na_{0.5}Bi_{0.5})_xBi_2Nb_2O_9$ solid solutions," *J. Adv. Ceram.*, vol. 3, no. 1, pp. 17–30, 2014.
[22] K. C. Kao, *Dielectric phenomena in solids*. Elsevier, 2004.
[23] O. Jongprateep, V. Petrovsky, and F. Dogan, "Effects of yttria concentration and microstructure on electric breakdown of yttria stabilized zirconia," *J. Met. Mater. Miner.*, vol. 18, no. 1, 2008.
[24] A. Padovani, D. Z. Gao, A. L. Shluger, and L. Larcher, "A microscopic mechanism of dielectric breakdown in SiO_2 films: An insight from multi-scale modeling," *J. Appl. Phys.*, vol. 121, no. 15, 2017.
[25] A. Bojovschi, T. V. Quoc, H. N. Trung, D. T. Quang, and T. C. Le, "Environmental effects on HV dielectric materials and related sensing technologies," *Appl. Sci.*, vol. 9, no. 5, p. 856, 2019.
[26] H. C. T. Fan, L. J. Ann, K. W. Loon, P. Y. Khai, R. A. Gamboa, and H. Ahmad, "Analysis of DC Breakdown Characteristics in Different Types Electrodes," *J. Eng. Sci. Technol. Spec. Issue SU18*, pp. 157–167, 2019.
[27] M. Meneghini, C. De Santi, I. Abid, M. Buffolo, M. Cioni, R. Abdul Khadar *et al.*, "GaN-based power devices: Physics, reliability, and perspectives," *J. Appl. Phys.*, vol. 130, no. 18, 2021.
[28] D. Mahdi, S. Zaidan, and M. Al-Hilli, "Homogeneity of Lithium Metasilicate-Copper Oxide Glass-Ceramics by Weibull Modulus," *J. Appl. Sci. Nanotechnol.*, vol. 1, no. 2, pp. 27–36, 2021.
[29] A. Andersen and J. R. Dennison, "Mixed Weibull distribution model of DC dielectric breakdowns with dual defect modes," in *2015 IEEE Conference on Electrical Insulation and Dielectric Phenomena (CEIDP)*, IEEE, 2015, pp. 570–573.
[30] K. Keshyagol, S. Hiremath, V. HM, and P. Hiremath, "Estimation of Energy Storage Capability of the Parallel Plate Capacitor Filled with Distinct Dielectric Materials," *Eng. Proc.*, vol. 59, no. 1, p. 95, 2023.
[31] T. M. Huber *et al.*, "Interplay of grain size dependent electronic and ionic conductivity in electrochemical polarization studies on Sr-doped LaMnO3 (LSM) thin film cathodes," *J. Electrochem. Soc.*, vol. 165, no. 9, p. F702, 2018.
[32] J. P. Gittings, C. R. Bowen, A. C. E. Dent, I. G. Turner, F. R. Baxter, S. Cartmell, *et al.*, "Influence of porosity on polarisation and electrical properties of hydroxyapatite based ceramics," *Ferroelectrics*, vol. 390, no. 1, pp. 168–176, 2009.
[33] Y. Slimani, A. Selmi, E. Hannachi, M. A. Almessiere, M. Mumtaz, A. Baykal, *et al.*, "Study of tungsten oxide effect on the performance of $BaTiO_3$ ceramics," *J. Mater. Sci. Mater. Electron.*, vol. 30, no. 14, pp. 13509–13518, 2019.
[34] C. Rayssi, S. El Kossi, J. Dhahri, and K. Khirouni, "Frequency and temperature-dependence of dielectric permittivity and electric modulus studies of the solid solution $Ca_{0.85}Er_{0.1}Ti_{1-x}Co_{4x/3}O_3$ ($0 \leq x \leq 0.1$)," *Rsc Adv.*, vol. 8, no. 31, pp. 17139–17150, 2018.
[35] S. Mahboob, Rizwana, G. Prasad, and G. S. Kumar, "Simulation of dielectric and resonance and anti-resonance data using modified Lorentz equation (T and ω simultaneously) of relaxor ferroelectric and

piezoelectric ceramics," *Bull. Mater. Sci.*, vol. 42, no. 2, p. 56, 2019.

[36] Y. Zhang, W. Li, S. Zhang, X. Tang, Q. Liu, Y. Jiang, *et al.*, "The dielectric relaxation and impedance spectroscopy analysis of $(Bi_{0.5}Na_{0.5})TiO_3$-based ceramics," *Mater. Res. Bull.*, vol. 153, p. 111874, 2022.

[37] A. Sati, A. Kumar, V. Mishra, K. Warshi, P. Pokhriyal, A. Sagdeo, *et al.*, "Temperature-dependent dielectric loss in $BaTiO_3$: Competition between tunnelling probability and electron-phonon interaction," *Mater. Chem. Phys.*, vol. 257, p. 123792, 2021.

[38] Y. Du, Y. Liu, Y. Yang, and L. Yang, "Recent advances in enhancing dielectric properties of CCTO materials via core-shell design strategies," *J. Alloys Compd.*, p. 181752, 2025.

[39] T. Wang, J. Hu, H. Yang, L. Jin, X. Wei, C. Li *et al.*, "Dielectric relaxation and Maxwell-Wagner interface polarization in Nb_2O_5 doped 0.65 $BiFeO_3$–0.35$BaTiO_3$ ceramics," *J. Appl. Phys.*, vol. 121, no. 8, 2017.

[40] A. Z. Al Ani and S. A. Zaidan, "Dielectric properties of polyester-nano tungsten oxide composites," in *AIP Conference Proceedings*, AIP Publishing LLC, 2024, p. 210004.

[41] D. M. D. M. Prabaharan, K. Sadaiyandi, M. Mahendran, and S. Sagadevan, "Structural, Optical, Morphological and Dielectric Properties of Cerium Oxide Nanoparticles," *Mater. Res.*, vol. 19, no. 2, pp. 478–482, Mar. 2016, doi: 10.1590/1980-5373-MR-2015-0698.

[42] M. Krichen, M. Megdiche, M. Gargouri, and K. Guidara, "Frequency and temperature dependence of the dielectric properties and AC electrical conductivity in mixed pyrophosphate ceramic," *Indian J. Phys.*, vol. 88, no. 10, pp. 1051–1058, 2014, doi: 10.1007/s12648-014-0552-0.

[43] J. Luo, E. F. Hairetdinov, D. P. Almond, and R. Stevens, "The characteristic frequencies for ionic conduction in 12 mol.% Y_2O_3 doped ZrO_2," *Solid State Ionics*, vol. 122, no. 1, pp. 205–210, 1999, doi: https://doi.org/10.1016/S0167-2738(99)00055-7.

[44] S. A. Zaidan, "Influence of Nano Barium-Titanate Glass Coating Layer on the Dielectric Properties of Zirconia," 2020.

[45] A. M. N. Lima, A. G. S. B. Neto, H. Neff, and E. U. K. Melcher, "Refined dielectric breakdown model for crystalline organic insulators: Electro-thermal instability coupled to interband impact ionization," in *2010 IEEE International Power Modulator and High Voltage Conference*, IEEE, 2010, pp. 63–68.

[46] S. Y. Lee, H. Kim, C. Baek, K. I. Park, G. J. Lee, S. H. Kim, *et al.*, "Yielding optimal dielectric energy storage and breakdown properties of lead-free pyrochlore ceramics by grain refinement strategies," *J. Alloys Compd.*, vol. 1008, p. 176569, 2024.